Relativistic Mean Field in $A \approx 80$ nuclei and low energy proton reactions

Chirashree Lahiri and G. Gangopadhyay

Department of Physics, University of Calcutta

92, Acharya Prafulla Chandra Road, Kolkata-700 009, India

Abstract

Relativistic Mean Field calculations have been performed for a number of nuclei in mass $A \approx 80$ region. Ground state binding energy, charge radius and charge density values have been compared with experiment. Optical potential have been generated folding the nuclear density with the microscopic nuclear interaction DDM3Y. S-factors for low energy (p, γ) and (p, n) reactions have been calculated and compared with experiment.

Relativistic Mean Field (RMF) approach has proved to be very successful in explaining different features of stable and exotic nuclei like ground state binding energy, deformation, radius, excited states, spin-orbit splitting, neutron halo, etc[1]. Particularly, the radius and the nuclear density are known to be well reproduced. Its has led to its application to nuclear reactions also.

Low energy reactions are very important from the astrophysical point of view. In astrophysical environments, neutron and proton reactions are the keys to nucleosynthesis of heavy elements. Mass 80 region is an interesting one as (p, γ) and (n, p) reactions play important roles in determining the abundance of elements. In this mass region, there are some proton-rich naturally occurring isotopes of elements known as p nuclei which can not be produced via s- or r- process. Mainly, proton capture reactions contribute to the formation of such nuclei. Recent works [See *e.g.* [2]] have emphasized the importance of a number of charge exchange reactions in this mass region for production of very light p nuclei. The relevant astrophysical rates can directly be derived from the (p, n) data, though the target is in the ground state and reaction has negative a Q-value[3]. A number of recent experiments has focussed on reactions using protons having a few MeV energy in mass 80 region.

Calculation of isotopic abundance requires a network calculation involving many thousands of reactions. Despite the importance of (p, γ) or (p, n) reactions in explaining the abundance of p nuclei, experimental data are rather scarce due unavailability of the target nuclei on earth. Thus, one often has to depend on theory for these reactions. The calculations essentially utilize the Hauser-Feshbach formalism where, the optical model potential, a key ingredient, is often taken in a local or a global form. It is also possible to use a microscopic optical potential constructed utilizing nuclear densities. If the target is stable, the density of the nucleus is available through electron scattering. However, in absence of stable target, theory remains our sole guide to describe the density. Thus, it is imperative to test the theoretical calculations, where experimental

data are available, to verify its applicability. We aim to to check the success of microscopic optical potentials based on mean field densities in explaining the reaction cross sections. A good description depending essentially on theory will allow one to extend the present method to the critical reactions which are beyond present day laboratory capabilities.

Calculations using microscopic potentials have been able to explain the observed elastic scattering cross sections even in nuclei far off the stability valley (See, *e.g.* Ref. [4] and references therein). Low energy projectiles probe only the outermost regions of the target nuclei. Hence, the nuclear skin plays a very important role in such reactions. The density information should be available from theoretical calculations. This method has been utilized to study low energy proton capture reactions in Ni and Cu nuclei[5] and nuclei in $A = 60 - 80$ region[6].

For the present study we have selected a number of low energy proton reactions for their astrophysical relevance. The reactions ^{84,86,87}Sr(p, γ) were investigated through activation technique by Gyürky *et al.* in Ref. [7]. It is important to note that ^{84}Sr is another p nucleus. In beam measurements were performed by Galanopoulos *et al.*[8] to find out the cross sections for the reaction ^{88}Sr(p, γ). As for charge exchange reactions, three reactions, identified as important by Rapp *et al.*[2] and for which experimental cross sections are available, have been selected for study. The reaction ^{75}As(p, n) was studied in [9, 10, 11] through in beam detection of neutrons. Finally, the reactions ^{76}Ge(p, n)[12] and ^{85}Rb(p, n)[3] were studied by activation technique. In the present work, we investigate the reactions mentioned above in a microscopic approach.

Theoretical density profiles were extracted in the RMF approach. There are different variations of the Lagrangian density as well as a number of different parametrizations. In the present work we have employed the FSU Gold[13] Lagrangian density. It contains, apart from the usual terms for a nucleon meson system, nonlinear terms involving self coupling of scalar-isoscalar meson, and additional terms describing self-coupling of the vector-isoscalar meson and coupling between the vector-isoscalar meson and the vector-isovector meson.

Pairing has been introduced under the BCS approximation using a zero range pairing force of strength 300 MeV-fm for both proton and neutrons. The RMF+BCS equations are solved under the usual assumptions of classical meson fields, time reversal symmetry, no-sea contribution, etc. Since we need the densities in co-ordinate space, the Dirac and the Klein Gordon equations have directly been solved in that space. This approach has earlier been used [4, 14, 15] in neutron rich nuclei in different mass regions.

The microscopic optical model potentials for the reactions are obtained using effective interactions derived from the nuclear matter calculation in the local density approximation, *i.e.* by substituting the nuclear matter density with the density distribution of the finite nucleus. In the present work, the microscopic nuclear potentials have been constructed by folding the density dependent DDM3Y[16, 17] effective interaction with the densities from the RMF calculation. This interaction, obtained from a finite range energy independent M3Y interaction by adding a zero range energy dependent pseudopotential and introducing a density dependent factor, has been employed successfully in nucleon nucleus as well as nucleus nucleus scattering, calculation of proton radioactivity, etc. The density dependence has been chosen in the form $C(1 - \beta \rho^{2/3})$[17], the

constants being obtained from a nuclear matter calculation[18]. The real and the imaginary parts of the potential are taken as 0.7 times and 0.1 times the DDM3Y potential, respectively. This normalization have also been used in our earlier work on (p, γ) reactions in lighter nuclei[6]. We have checked that the above values adequately describe the cross section measurements. Of course, these parameters can be tuned to fit the cross sections in individual reactions. For example, in ^{84}Sr, if we choose the imaginary part of the potential as 0.3 times of the DDM3Y potential, the result will differ by 10% and fit the experimental data better. However, we believe a single parametrization for the entire mass region to be more useful.

The Coulomb potentials are similarly constructed by folding the Coulomb interaction with the microscopic proton densities. We have already used such potentials to calculate life times for proton, alpha and cluster radioactivity[19] as well as elastic proton scattering[4] in different mass regions of the periodic table.

Reaction calculations have been performed with the computer code TALYS 1.2[20] assuming spherical symmetry for the target nuclei. DDM3Y interaction is not a standard input of TALYS but can easily be incorporated. Though the nuclear matter-nucleon potential does not include a spin-orbit term, the code provides a spin-orbit potential from the Scheerbaum prescription[21] coupled with the phenomenological complex potential depths. The default form for this potential given in the code has been used without any modification.

The TALYS code has a number of other useful features. We have employed the full Hauser-Feshbach calculation with transmission coefficients averaged over total angular momentum values and with corrections due to width fluctuations. Up to thirty discrete levels of the nuclei involved have been included in the calculation.

Our calculations, being more microscopic, are more restricting. Yet, the rate depends on the models of the level density and the E1 gamma strength function adopted in the calculation of cross sections. Phenomenological models are usually fine tuned for nuclei near the stability valley. Microscopic prescriptions, on the other hand, can be extended to the drip lines, and hence, have been assumed in all nuclei. We have calculated our results with microscopic level densities in Hartree-Fock (HF) and Hartree-Fock-Bogoliubov (HFB) methods, calculated in TALYS by Goriley and Hilaire, respectively. We have also compared our results using phenomenological level densities from constant temperature Fermi gas model, back shifted Fermi gas model and generalised superfluid model from TALYS. The cross sections are very much dependent on the level density chosen, sometimes changing by a factor of 50%. We find that in most of the cases, the HFB densities fit the experimental data better in our formalism.

For E1 gamma strength functions, results derived from HF+BCS and HFB calculations, available in the TALYS data base, have been employed. In agreement with our observation in in [6], here also the results for HFB calculations describe the S-factors reasonably well and we present our results for that approach only.

It is possible to scale the theoretical capture cross sections to match with experiment using a parameter G_{norm} in the code used to scale the gamma-ray transmission coefficient. However, for the present paper, we have not scaled the theoretical results. All the parameters in the Lagrangian density and the interaction are standard ones and have not been changed.

As the density profile is the important quantity in our formalism, a comparison of the radii values can provide some idea about the agreement of the calculated densities with experiments. In Table 1, we compare our results for the binding energy and charge radii (r_{ch}) with measurements for those nuclei in this mass region, which have been used as targets for low energy proton capture or charge exchange reactions. The binding energy values from the mean field approach have been corrected using the formalism developed in [22, 23]. The experimental binding energy values are from Ref. [24].

Charge radii have been calculated from the charge densities, which, in turn, have been obtained from the calculated point proton density ρ_p by taking into account the finite size of the proton. The point proton density is convoluted with a Gaussian form factor $g(\mathbf{r})$,

$$\rho_{ch}(\mathbf{r}) = \int e\rho_p(\mathbf{r'})g(\mathbf{r} - \mathbf{r'})d\mathbf{r'} \tag{1}$$

$$g(\mathbf{r}) = (a\sqrt{\pi})^{-3}\exp(-r^2/a^2) \tag{2}$$

with $a = 0.8$ fm.

Experimental charge radii values are from Angeli[25]. The results show that RMF can describe the charge radii of these nuclei with sufficient accuracy. One sees that in most of the nuclei, the difference between measurement and theory is less than 1%.

Direct comparison of charge density is more difficult in absence of accurate experimental information. De Vries *et al.*[26] have presented the coefficients of Fourier-Bessel expansion for charge density of a number on nuclei extracted from electron scattering data. It includes two nuclei of our interest, ^{76}Ge and ^{88}Sr. In Fig. 1, we compare the charge density extracted from the Fourier-Bessel coefficients and our calculated results for the above two nuclei. One can see that the theoretical and experimental values agree very well, particularly at larger radii values, which is the region expected to contribute to the optical potential at low projectile energy. However, in absence of information on error in the density values, this conclusion can remain only tentative.

Next, we compare the results for the reaction calculation in the above mentioned reactions with experiments. As the astrophysically important Gamow window lies in the region 1.3 to 3.9 MeV for these nuclei, we present the results covering this energy region. The cross-section varies very rapidly at such low energy making comparison between theory and experiment rather difficult. The usual practice in low energy nuclear reaction is to compare another key observable, *viz.* S-factor. The expression of the astrophysical S-factor[6] is given by,

$$S(E) = E\sigma(E)e^{2\pi\eta} \tag{3}$$

where E is the energy in centre of mass frame in KeV, $\sigma(E)$ is reaction cross-section in barn and η indicates the Sommerfeld parameter which may be obtained from the relation, $2\pi\eta = 31.29 Z_p Z_t \sqrt{\mu/E}$. Here, Z_p and Z_t are the charge numbers of the projectile and the target, respectively and μ is the reduced mass (in amu). It varies much slowly than reaction cross-sections as the exponential energy dependence of cross-section is not present in it. For this reason, we calculate this quantity and compare it with experimentally extracted values.

Figures 2 and 3 show the results for the reactions $^{84,86-88}$Sr(p, γ). The results compare favourably with experiments compared to the NON-SMOKER code calculations of Rauscher *et al.*[27]. However, it needs to be pointed out that, in the case of ^{87}Sr, theoretical results overpredict the cross section values. It was suggested[7] that perhaps the agreement with theory (in their case the NON-SMOKER calculation) worsens as one goes to more neutron-rich nuclei. However, as one can see in the right panel of Figure 2, this trend is not shared by the present calculation.

Figure 3 shows the results for the (p, n) reactions on (a) ^{75}As, (b) ^{76}Ge and (c) ^{85}Rb targets. These reactions (along with their inverse reactions) are listed among the ten most important reactions in deciding the abundance of the p nuclei in Rapp *et al.*[2]. The three measurements for the ^{75}As(p, n) reaction are rather old and error values are not available for most of the measurements. The quoted error in cross section is 10% or above. In ^{76}Ge, we find that the calculation systematically overpredict the results by as much as 60%. On the other hand, the calculations for the ^{85}Rb(p, n) reaction produce excellent match with experimental measurements.

We find that our calculation can reproduce the S-factor values with reasonable success. Even in the worst case, calculation is off by a factor less than two while the cross section values range over four orders of magnitude. However, one should remember that in astrophysical calculations, the rates are often varied by a large factor, *viz.* ten or hundred[2]. Thus the present microscopic calculations can be used to obtain rates which are dependable for astrophysical calculations.

We point out that in our earlier work[5], we have seen that the default local and global optical potentials [28] in the TALYS package also can be used with suitable normalization of gamma ray strength to produce comparable results for certain energy ranges. In the present case also, suitable selection of the parameter brings the values calculated with default potential close to experimental values. However, we believe that the present microscopic approach is more suitable as no normalization is necessary and the method can be extended to reactions where experimental data are not available.

In summary, cross sections for low energy (p, γ) and (p, n) reactions for a number of nuclei in mass 80 region in the energy regime important for explosive nucleosynthesis have been calculated using the TALYS code. The microscopic optical potential has been obtained by folding the DDM3Y microscopic interaction with the nuclear densities obtained from RMF calculation using the Lagrangian density FSU Gold.

References

[1] See *e.g.* P. Ring, Prog. Part. Nucl. Phys **37**, 193 (1996).

[2] W. Rapp *et al.*, Astrophys J. **653**, 474 (2006).

[3] G.G. Kiss *et al.*, Phys. Rev. Lett. **101**, 191101 (2008). T. Rauscher *et al.*, Phys. Rev. C **80**, 035801 (2009).

[4] G. Gangopadhyay and S. Roy J. Phys. G: Nucl. Part. Phys. **31**, 1111 (2005).

[5] G. Gangopadhyay, Phys. Rev. C **82**, 027603 (2010).

[6] C. Lahiri and G. Gangopadhyay, Eur. Phys. J. A **47**, 87 (2011).

[7] Gy. Gyürky *et al.*, Phys. Rev. C **64**, 065803 (2001).

[8] S. Galanopoulos *et al.*, Phys. Rev. **67**, 015801 (2003).

[9] C.H. Johnson, A. Galonsky, and J.P. Ulrich, Phys. Rev. **109**, 1243 (1958).

[10] C.H. Johnson, C. Trail, and A. Galonsky, Phys. Rev. **136**, B1719 (1964).

[11] R.D. Albert, Phys. Rev. **115**, 925 (1959).

[12] G.G. Kiss *et al.*, Phys. Rev. C **76**, 055807 (2007).

[13] J. Piekarewicz and B.G. Todd-Rutel, Phys. Rev. Lett. **95**, 122501 (2005).

[14] M. Bhattacharya and G. Gangopadhyay, Phys. Rev. C **72**, 044318 (2005); Fizika B **16**, 113 (2007).

[15] M. Bhattacharya and G. Gangopadhyay, Phys. Rev. C **75**, 017301 (2007).

[16] A.M. Kobos *et al.*, Nucl. Phys. **A425**, 205 (1984).

[17] A.K. Chaudhuri Nucl. Phys. **A449**, 243 (1986); **A459**, 417 (1986)

[18] D.N. Basu, J. Phys. G: Nucl. Part. Phys. **30**, B7 (2004).

[19] G. Gangopadhyay, J. Phys. G: Nucl. Part. Phys. **36**, 095105 (2009) and references therein.

[20] A.J. Koning, S. Hilaire, and M. Duijvestijn, Proceedings of the International Conference on Nuclear Data for Science and Technology, April 22-27, 2007, Nice, France, editors Bersillon O, Gunsing F, Bauge E, Jacqmin R, and Leray S, EDP Sciences, 2008, p. 211-214.

[21] R.R. Scheerbaum, Nucl. Phys. **A257**, 77 (1976).

[22] M. Bhattacharya and G. Gangopadhyay, Phys. Lett. B **672**, 182 (2009).

[23] G. Gangopadhyay, J. Phys. G : Part. Nucl. Phys **37**, 015108 (2010).

[24] G. Audi, A.H. Wapstra and C. Thibault, Nucl. Phys. **A729**, 337 (2003).

[25] I. Angeli, At. Data Nucl. Data Tables **87**, 185 (2004).

[26] H. De Vries, C.W. De Jager and C. De Vries, At. Data Nucl. Data Tables **36**, 495 (1987).

[27] T. Rauscher and F.-K. Thielmann, At. Data Nucl. Data Tables **75**, 1 (2000); **76**, 47 (2001).

[28] A.J. Koning and J.P. Delaroche, Nucl. Phys. **A713**, 231 (2003).

Table 1: Experimental binding energy and charge radii values compared with calculated results.

	B.E.(MeV)		r_{ch}(fm)	
	Exp.	Theo.	Exp.	Theo.
^{84}Sr	728.90	727.53	4.236	4.232
^{86}Sr	748.93	748.27	4.226	4.240
^{87}Sr	757.36	757.17	4.220	4.245
^{88}Sr	768.47	768.47*	4.220	4.249
^{75}As	652.56	652.38	4.097	4.082
^{76}Ge	661.60	660.69	4.081	4.053
^{85}Rb	739.28	738.70	4.203	4.218

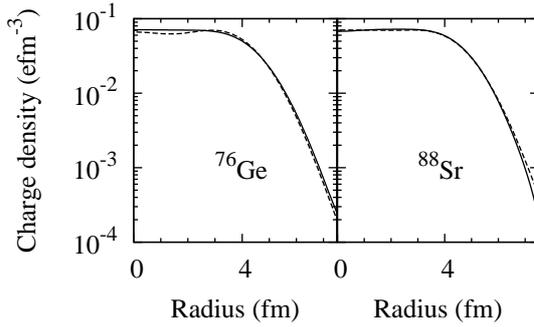* Normalized following the prescription of [22, 23].

Figure 1: Comparison of charge density obtained from Fourier-Bessel analysis of experimental electron scattering data (solid line) and calculated in the present work (dashed line).
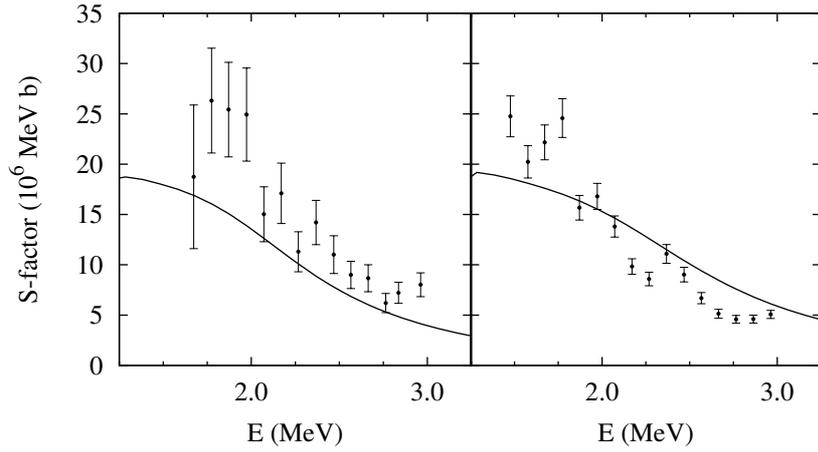
Figure 2: Experimental and calculated S-factors for (p, γ) reactions in (a)^{84}Sr and (b) ^{86}Sr targets.
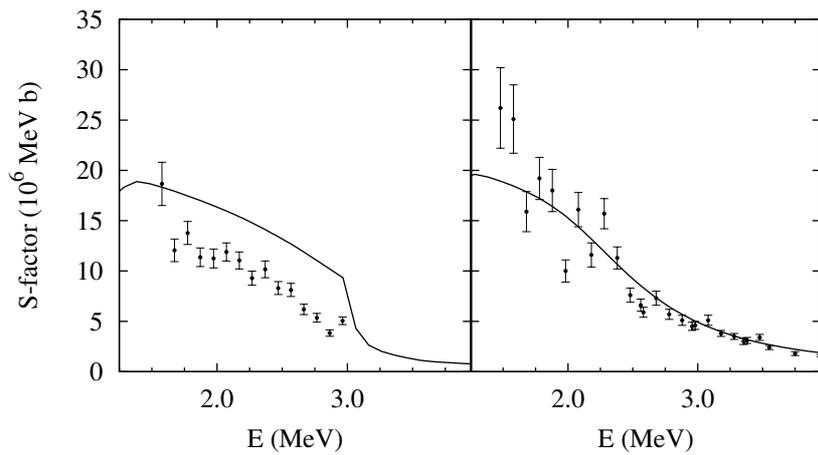

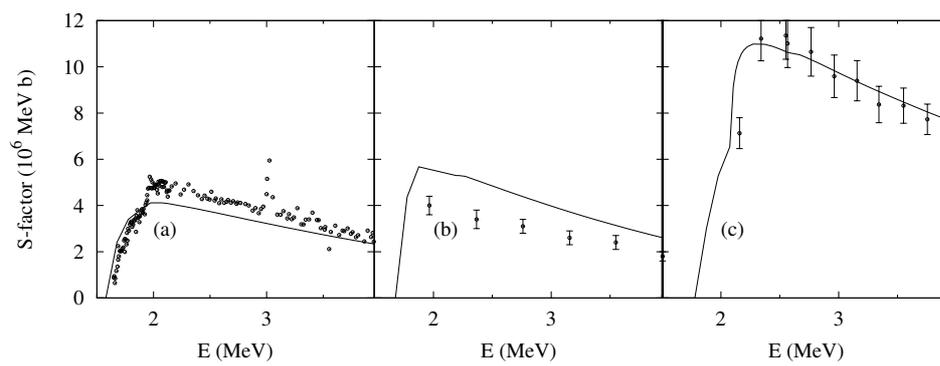Figure 3: Experimental and calculated S-factors for (p, γ) reactions in (a)^{87}Sr and (b) ^{88}Sr targets.

Figure 4: Experimental and calculated S-factors for (a) ^{75}As(p, n), (b) ^{76}Ge(p, n) and (c) ^{85}Rb(p, n) reactions, respectively.